AMERICAN SOCIETY FOR MICROBIOLOGY | Journal of Bacteriology

csrT Represents a New Class of *csrA*-Like Regulatory Genes Associated with Integrative Conjugative Elements of *Legionella pneumophila*

Zachary D. Abbott,[a]* Kaitlin J. Flynn,[a] Brenda G. Byrne,[a] Sampriti Mukherjee,[b]* Daniel B. Kearns,[b] Michele S. Swanson[a]

Department of Microbiology and Immunology, University of Michigan Medical School, Ann Arbor, Michigan, USA[a]; Department of Biology, Indiana University, Bloomington, Indiana, USA[b]

ABSTRACT

Bacterial evolution is accelerated by mobile genetic elements. To spread horizontally and to benefit the recipient bacteria, genes encoded on these elements must be properly regulated. Among the legionellae are multiple integrative conjugative elements (ICEs) that each encode a paralog of the broadly conserved regulator *csrA*. Using bioinformatic analyses, we deduced that specific *csrA* paralogs are coinherited with particular lineages of the type IV secretion system that mediates horizontal spread of its ICE, suggesting a conserved regulatory interaction. As a first step to investigate the contribution of *csrA* regulators to this class of mobile genetic elements, we analyzed here the activity of the *csrA* paralog encoded on *Legionella pneumophila* ICE-βox. Deletion of this gene, which we name *csrT*, had no observed effect under laboratory conditions. However, ectopic expression of *csrT* abrogated the protection to hydrogen peroxide and macrophage degradation that ICE-βox confers to *L. pneumophila*. When ectopically expressed, *csrT* also repressed *L. pneumophila* flagellin production and motility, a function similar to the core genome's canonical *csrA*. Moreover, *csrT* restored the repression of motility to *csrA* mutants of *Bacillus subtilis*, a finding consistent with the predicted function of CsrT as an mRNA binding protein. Since all known ICEs of legionellae encode coinherited *csrA*-type IV secretion system pairs, we postulate that CsrA superfamily proteins regulate ICE activity to increase their horizontal spread, thereby expanding *L. pneumophila* versatility.

IMPORTANCE

ICEs are mobile DNA elements whose type IV secretion machineries mediate spread among bacterial populations. All surveyed ICEs within the *Legionella* genus also carry paralogs of the essential life cycle regulator *csrA*. It is striking that the *csrA* loci could be classified into distinct families based on either their sequence or the subtype of the adjacent type IV secretion system locus. To investigate whether ICE-encoded *csrA* paralogs are bona fide regulators, we analyzed ICE-βox as a model system. When expressed ectopically, its *csrA* paralog inhibited multiple ICE-βox phenotypes, as well as the motility of not only *Legionella* but also *Bacillus subtilis*. Accordingly, we predict that CsrA regulators equip legionellae ICEs to promote their spread via dedicated type IV secretion systems.

Mobile DNA elements can spread advantageous traits among bacterial populations and contribute to the evolution of pathogens (1). Integrative conjugative elements (ICEs) are one type of mobile transposable element that encode their own type IV secretion system (T4SS) for transfer between strains and also the enzymes necessary to integrate the element into the host chromosome. ICEs have expanded the genetic repertoire of a number of bacterial pathogens by carrying a variety of cargo genes that confer advantageous traits for their hosts, enhancing fitness in specific environments. Some ICEs provide resistance to antibiotics, metal ions, and oxidative stress; others enhance nitrogen and chlorobenzoate metabolism, biofilm formation, and host cell infection (2–5). In addition to cargo genes are those encoding the elements' structural components. Multiple distinct classes of T4SSs mediate ICE transmission within and between species (6). This diversity may permit multiple ICEs to persist within one cell, since bacteria typically maintain only one of each T4SS type (7).

Bacteria coordinate expression of multiple extracellular structures, each with distinct purposes. *L. pneumophila* produces short pili for adherence or long T4SS conjugative pili for effector secretion or horizontal gene transfer but not both pili at the same time (8). Indeed, simultaneous expression of similar T4SS by *L. pneumophila* appears to be counterproductive, as activity of the core Dot/Icm T4SS is inhibited by the MobA component of a related RSF1010 conjugative plasmid (9). Accordingly, competition between ICEs likely provides selective pressure for regulatory circuits that ensure reciprocal expression of their T4SS machines.

The regulatory mechanisms governing the expression of ICE traits are as diverse as the ICEs themselves. For example, SXT from *Vibrio cholerae* and ICEBs1 from *B. subtilis* encode regulatory proteins that are cleaved or bound by host regulators induced by the bacterial SOS response (2, 10). Other ICEs are equipped with reg-

Received 31 August 2015 **Accepted** 12 November 2015

Accepted manuscript posted online 23 November 2015

Citation Abbott ZD, Flynn KJ, Byrne BG, Mukherjee S, Kearns DB, Swanson MS. 2016. *csrT* represents a new class of *csrA*-like regulatory genes associated with integrative conjugative elements of *Legionella pneumophila*. J Bacteriol 198:553–564. doi:10.1128/JB.00732-15.

Editor: I. B. Zhulin

Address correspondence to Michele S. Swanson, mswanson@umich.edu.

* Present address: Zachary D. Abbott, Biorasi, Miami, Florida, USA; Sampriti Mukherjee, Department of Molecular Biology, Princeton, New Jersey, USA.

Z.D.A. and K.J.F. contributed equally to this article.

Supplemental material for this article may be found at http://dx.doi.org/10.1128/JB.00732-15.

ulatory circuitries that act independently of host proteins. ICEclc from *Pseudomonas aeruginosa* and CTnDOT from *Bacteroides thetaiotaomicron* carry sensor proteins that respond to chlorobenzoate or tetracycline, respectively; these chemicals induce transcription of regulatory genes that drive expression of cargo loci that confer protection from these stressors (11, 12). The ICEs pLS20 from *B. subtilis* and pAD1 of *Enterococcus faecalis* rely on secreted peptides or pheromones to sense recipient cells in the environment and induce a signaling cascade that activates transcription of the conjugative pilus (13, 14). Finally, to regulate transfer, the *Agrobacterium tumefaciens* Ti conjugative plasmid responds to the secreted quorum sensing *N*-acyl-L-homoserine lactone molecule (15). In these ways, each regulatory system specifically activates ICE traits.

The environmental and opportunistic pathogen *L. pneumophila* carries multiple ICEs in its genome. For instance, the Philadelphia-1 strain of *L. pneumophila* harbors three distinct ICEs (16). One of these mobile elements, ICE-βox, enhances the pathogen's resistance to bleach and the β-lactam antibiotics oxacillin and penicillin (4). Strains that carry ICE-βox are also more infectious and tolerant of the macrophage phagocyte oxidase (4). Protecting the bacterium from these stresses presumably benefits ICE-βox by ensuring a healthy host competent for spread of the element. Thus, expression of the ICE-βox-encoded T4SS transmission machinery and cargo traits must be regulated in a manner that ensures ICE-βox maintenance in bacterial populations.

ICE-βox encodes a paralog of *csrA*, an essential regulator of *L. pneumophila* differentiation. The canonical CsrA is encoded in the "core" genome: the gene is ubiquitous and highly conserved in the *Legionella* genus and is not encoded within a horizontally acquired genetic element (17, 18). CsrA is an mRNA binding protein that is essential for *L. pneumophila* replication and represses numerous *L. pneumophila* transmissive-phase traits, including expression of substrates of the core Dot/Icm T4SS (19, 20). Similar to the dual CsrA system in *P. aeruginosa* (21), CsrA binds and represses expression of the mRNA encoding *csrR*, a newly identified *csrA* paralog in the *L. pneumophila* core genome, a design predicted to establish reciprocal expression profiles (22).

The legionellae also encode a large "accessory" genome: highly variable regions of the genome frequently composed of horizontally acquired elements, including ICEs, that are not conserved between strains and species (17, 18, 23–25). The ICE Trb-1 mobile element of *L. pneumophila* strain Corby also encodes a *csrA* paralog, *lvrC* (26). Mobility of ICE Trb-1 is repressed in laboratory conditions, as deletion of the *lvrRABC* regulatory region significantly increases the number of episomal ICE Trb-1 copies (26). No host phenotypic advantages of harboring ICE Trb-1 have been identified; thus, whether *lvrRABC* also regulates ICE Trb-1 cargo genes remains to be determined.

Because a paralog of the known pluripotent regulator *csrA* is found in every known *L. pneumophila* ICE, we sought to determine whether ICE *csrA* paralogs retain function as regulators. Given the observations that canonical CsrA represses multiple traits mediated by the core Dot/Icm T4SS (19, 20) and that ICE Trb-1 mobility is repressed by its *lvrRABC* locus (26), we investigated whether *csrT*, the *csrA* paralog on ICE-βox, is competent to regulate traits encoded by either its mobile element or the core *L. pneumophila* genome.

MATERIALS AND METHODS

Bacterial strains, culture conditions, and reagents. *Legionella pneumophila* strains were cultured in *N*-(2-acetamido)-2-aminoethanesulfonic acid (ACES; Sigma)-buffered yeast extract (AYE) broth supplemented with 100 μg/ml thymidine (AYET; Sigma) at 37°C. CFU were identified by plating on ACES-buffered charcoal yeast extract agar (CYE) supplemented with thymidine (CYET) and incubated at 37°C for 4 days (27). Bacteria cultured overnight in AYET were diluted and incubated overnight to obtain cells in exponential (E; optical density at 600 nm [OD_{600}] of 1.2 to 1.8) or postexponential (PE; OD_{600} of 2 to 3.7) phases. When necessary for mutant or plasmid selection, the following antibiotics were added: gentamicin (Gibco) at 10 μg/ml, kanamycin (Kan; Sigma) at 25 μg/ml, or chloramphenicol (Cam; Fisher) at 5 μg/ml. IPTG (isopropyl-β-D-thiogalactopyranoside; Gold Biotechnology) was added to a final concentration of 200 μM unless otherwise indicated. Hydrogen peroxide (Sigma) was diluted in AYET to a final concentration of 2 mM. Strains, plasmids, and primers used in this study are summarized in Table S1 in the supplemental material.

Phylogeny and alignment. The predicted amino acid sequences of the 34 ICE-associated *csrA* paralogs (see Table S2 in the supplemental material) were aligned using ClustalW2 (28). The alignment was used to generate a maximum-likelihood phylogenetic tree with PhyML using the LG substitution model, four substitution rate categories, and 100 bootstraps (29). The resulting tree was visualized using iTOL (30).

Using the order of *csrA* paralogs determined from the phylogeny, pairwise alignment of the T4SSs were generated using tBLASTx and EasyFig (31). Nucleotide sequences of the T4SS and annotation were taken directly from the NCBI Nucleotide database (see Table S3 in the supplemental material).

Induced expression constructs. Wild-type (WT) *csrA* (*lpg0781*), *csrT* (*lpg2094*), and *csrA-22* (*lpg1003*) with C-terminal His_6 tags were amplified from Lp02 genomic DNA using the primer sets ZA33+34, ZA11+12, and ZA15+16, respectively. The resultant PCR products were digested with SalI and HindIII and ligated into p206gent (32). These plasmids were then electroporated into Lp02 to generate strains MB1389, MB1383, and MB1435. We verified that adding 200 μM IPTG resulted in protein expression (data not shown) by Western analysis using a 1:5,000 dilution of anti-His(C-term)-horseradish peroxidase (HRP)-conjugated antibody and the Western blot protocol described below.

Δ*csrT* mutant construction. A *csrT* mutant was generated via recombineering as described previously (33). The *csrT* coding sequence plus its 500-bp 5′ and 3′ flanking region was amplified using primers (KF67 and KF70) (see Table S1 in the supplemental material). The resulting fragment was cloned into pGEM-T Easy (Promega) and electroporated into *Escherichia coli* DY330 where λ-red recombinase replaced the *csrT* region with a gentamicin (Gm) resistance cassette. The recombinant alleles were transformed into strain Lp02 (MB110) or Lp02 containing a marked ICE-βox (MB1353) to generate Δ*csrT* mutant strains MB1409 and MB1507, respectively. Insertion of the mutant allele was confirmed by selection on CYET-Gm and screening by PCR.

Mice. Six- to eight-week-old female A/J mice were purchased from Jackson Laboratories. Mice were housed in the University Laboratory Animal Medicine Facility at the University of Michigan Medical School under specific-pathogen-free conditions. The University Committee on Use and Care of Animals approved all experiments conducted in this study.

Hydrogen peroxide exposure assay. Stress resistance was assessed by quantifying bacterial CFU after exposure to hydrogen peroxide. E-phase strains containing pcsrT (MB1383, MB1384, and MB1385) were cultured in AYET with or without IPTG induction overnight. After subculture to an OD_{600} of 1.0, cultures were treated with 2 mM H_2O_2 for 1 h at 37°C. The mean ± the standard error of the mean (SEM) percent survival was calculated from triplicate samples.

Intracellular growth and immunofluorescence microscopy. Growth of bacteria in bone marrow-derived macrophages from A/J mice (Jackson Laboratories) was assessed as described previously (34). Strains were cul-

tured to the PE phase with or without 200 μM IPTG overnight prior to infection. To achieve a similar multiplicity of infection (MOI), uninduced motile strains were added at bacteria/host ratio of 1, while induced nonmotile strains were added at ratio of 2. For induced samples, IPTG was included in the infection media at a concentration of 1 mM as described previously (19). Infection efficiency was calculated as follows: (macrophage-associated CFU at 90 min postinfection/input CFU) × 100.

Microscopy was performed by plating 3×10^5 macrophages on 12-mm glass coverslips overnight prior to infection with bacteria cultured as described above. At 90 min postinfection, macrophages were fixed and stained as described previously (35) using a 1:50 dilution of *L. pneumophila* primary antibody obtained from mouse monoclonal hybridoma cell line CRL-1765 (ATCC) and a 1:1,000 dilution of anti-mouse IgG antibody conjugated to Oregon Green (Molecular Probes). To quantify colocalization with the late endosomal and lysosomal marker LAMP-1, fixed macrophages were stained with a 1:500 dilution of rat anti-LAMP-1 (Santa Cruz) and a 1:1,000 dilution of anti-rat IgG antibody conjugated to Oregon Green (Molecular Probes). The DNA stain DAPI (4′,6′-diamidino-2-phenylindole) was applied in the ProLong Gold antifade reagent (Molecular Probes) used as a mounting medium. Scoring of degraded or LAMP-1-colocalized bacteria was performed by assessing 30 to 50 bacteria per coverslip in triplicate. NADPH oxidase experiments were performed using the pair of cell lines J774.16 (WT) and J774.D9 *phox* (deficient in gp91 subunit of NADPH oxidase) that were infected as described above (36).

Generation of marked LpgGI-1 strain. The marked LpgGI-1 strain was generated by recombineering as described previously (4). The noncoding region between *lpg1009* and *lpg1010* was amplified by PCR using the primers 5′-CTGCGCCTACGTAAAACCC-3′ (forward, KF47) and 5′-GCAGACATGGGAGCGAG-3′ (reverse, KF50) and cloned into pGEM-T Easy (Promega). After electroporation into *E. coli* strain DY330, λ-red recombinase replaced the ICE-ice noncoding region with a kanamycin (Kan) resistance cassette as described previously (33). The recombinant alleles were transferred to strain Lp02 via natural transformation to generate strain MB1398. Insertion of the Kan cassette was confirmed by selection on CYET-Kan and by PCR.

Construction of donor strains for conjugation. Strains containing the marked ICEs and the plasmids with IPTG-inducible *csrT* or *csrA-22* genes were generated by mating as described previously (4, 37). Briefly, a culture of a strain with a marked ICE was mixed with a culture of the strain carrying a *csr* plasmid on CYET agar and incubated at 37°C for 2 h. The cell mixture was then transferred to CYET agar with appropriate antibiotics to select for isolates with the desired marked ICE and *csr* expression plasmid. Strains were confirmed by isolation streaking two times on CYET agar with appropriate antibiotics and by PCR.

Conjugation. To analyze ICE-βox transfer by conjugation, the following thymidine auxotroph donor strains, each containing a chloramphenicol-resistance marked ICE-βox, were used: Lp02 (MB1353), *csrT* mutant (MB1507), Lp02/pcsrT (MB1465), and Lp02/pcsrA-22 (MB1499). Similarly, to analyze LpgGI-1 transfer by conjugation, the following thymidine auxotroph donor strains, each containing a Kan resistance marked LpgGI-1, were used: Lp02 (MB1398), Lp02/pcsrT (MB1500), and Lp02/pcsrA-22 (MB1501). Each donor strain was cultured in AYE with or without IPTG overnight to E phase. As a recipient, the thymidine prototroph JR32 (MB370) was also cultured in AYE overnight to E phase. 10^9 donor cells were mixed with 10^{10} recipient cells on 0.22-μm-pore-size filters (Millipore) placed on prewarmed CYET agar plates and incubated at 37°C for 2 h as described previously (4, 37). For strains in which ectopic *csr* expression was induced, 10 μl of 200 mM IPTG was placed under the filter. Serial dilutions of the mating mixture were plated on CYET-Cam (5 μg/ml) to select for donors and CYE-Cam to select for transconjugants. The transconjugation efficiency was calculated as $(CFU_{transconjugants}/CFU_{donor\ cells}) \times 100$ in triplicate from three independent experiments.

Motility and flagellin analysis. Wild-type (MB110), Δ*flaA* mutant (MB1390), and strains carrying pcsrA and pcsrT (MB1389 and MB1383) were cultured in AYET to E phase and then diluted to an OD_{600} of 0.2. Strains MB1389 and MB1383 were each divided between two tubes, and one was induced with 200 μM IPTG. Next, all strains were cultured at 37°C for ~15 h to PE phase, and then motility was assessed qualitatively by observation of wet mounts by inverted phase microscopy. Aliquots of the cultures were subsequently normalized to an OD_{600} of 10 and then resuspended in 100 μl of Laemmli buffer (2% sodium dodecyl sulfate, 10% glycerol, 5% 2-mercaptoethanol, 0.005% bromophenol blue, 62.5 mM Tris-HCl [pH 6.8]). Samples were lysed by boiling for 5 min, and debris was pelleted at 13,000 rpm for 2 min. Proteins were separated on a 12% mini-Protean TGX precast gel (Bio-Rad), and a Precision Plus Kaleidoscope protein standard ladder (Bio-Rad) was used as a size marker and to verify transfer. To assess equal loading and transfer of each sample, Ponceau-S (Fisher) staining was performed on a duplicate membrane. Flagellin was detected using a 1:100 dilution of 2A5 rabbit monoclonal antibody (a gift from N. C. Engelberg, University of Michigan Medical School), a 1:3,000 dilution of goat anti-rabbit secondary IgG–HRP (Pierce), and the SuperSignal West Pico chemiluminescent substrate (Thermo Scientific).

***Bacillus subtilis* culture.** *B. subtilis* strains were cultured in Luria-Bertani (LB; 10 g of tryptone, 5 g of yeast extract, and 5 g of NaCl per liter) broth or on LB plates fortified with 1.5% Bacto agar at 37°C. When appropriate, antibiotics were included at the following concentrations: 10 μg/ml tetracycline, 100 μg/ml spectinomycin, 5 μg/ml chloramphenicol, 5 μg/ml kanamycin, and 1 μg/ml erythromycin plus 25 μg/ml lincomycin. Finally, 1 mM IPTG (Sigma) was added to the medium when appropriate.

***B. subtilis* strain construction.** To generate the *amyE*::$P_{hyspank}$-*csrALp* spec complementation construct, PCR product containing the *csrALp* coding region was amplified from *L. pneumophila* chromosomal DNA using the primer pair 3520/3521. DNA fragments containing the IPTG-inducible $P_{hyspank}$ promoter, a spectinomycin resistance cassette, and the *amyE* region was amplified from the strain DS4940 as the template using the primers 3177/3519 and 3170/3180. Next, the PCR products were ligated using Gibson assembly (38). The complementation constructs *amyE*::$P_{hyspank}$-*csrX* spec, *amyE*::$P_{hyspank}$-*csrT* spec, *amyE*::$P_{hyspank}$-*csrA-22* spec, and *amyE*::$P_{hyspank}$-*lvrC* spec were generated in a similar way using PCR amplicons from *L. pneumophila* chromosomal DNA using the primer pairs 3522/3523, 3524/3525, 3526/3527, and 3528/3529, respectively.

All constructs were first introduced into the domesticated strain DS2569 by natural competence and then transferred to the 3610 and DS6530 background using SPP1-mediated generalized phage transduction (39).

***B. subtilis* swarm expansion assay.** Cells were cultured to mid-log phase at 37°C in LB and resuspended to an OD_{600} of 10 in pH 8.0 PBS buffer (137 mM NaCl, 2.7 mM KCl, 10 mM Na_2HPO_4, and 2 mM KH_2PO_4) containing 0.5% India ink (Higgins). Freshly prepared LB medium containing 0.7% Bacto agar (25 ml/plate) was dried for 20 min in a laminar flow hood, centrally inoculated with 10 μl of the cell suspension, dried for another 10 min, and incubated at 37°C. The India ink demarks the origin of the colony, and the swarm radius was measured relative to the origin. For consistency, an axis was drawn on the back of the plate and swarm radii measurements were taken along this transect. For experiments including IPTG, cells were propagated in broth in the presence of IPTG, and IPTG was included in the swarm agar plates.

RESULTS

***csrA* paralogs and their associated T4SSs are genetically linked.** The *Legionella* pan-genome has been predicted or demonstrated to encode many ICEs (4, 40, 41). In each of the 34 legionellae ICEs identified (see Table S3 in the supplemental material), a *csrA*-like gene immediately precedes the locus encoding the T4SS. Previously, we identified distinct families of *csrA*-like genes based on their amino acid sequence similarity (22). Likewise, *Legionella*

ICEs encode several different lineages of T4SSs (4, 26, 41–43). Therefore, we investigated whether particular lineages of ICE-encoded T4SSs were genetically linked to a distinct *csrA* paralog. To do so, we first determined the relationship of all 34 *csrA* paralogs (see Table S2 in the supplemental material) by generating a phylogenetic tree (Fig. 1A). Four distinct groups were apparent based on their amino acid sequence; only 5 of the 34 paralogs did not clearly fall into any group.

To determine whether the T4SS lineages paired with a specific group of *csrA* paralogs, we next aligned the T4SSs associated with each of the *csrA* paralogs. Indeed, within each *csrA* paralog group, the associated T4SSs lineages were quite similar, whereas there was little similarity between T4SSs that are genetically linked to different *csrA* families (Fig. 1B). For instance, all the T4SSs associated with *csrA* paralogs in group IV aligned strongly and indeed included every T4SS in the LGI lineage identified by Wee et al. (41). On the other hand, the T4SSs in *csrA* group IV did not align with those of the Trb T4SS lineage (group I [42]), the Tra T4SS lineage (group II [4]), or the Lvh T4SS lineage (group III [43]). Whereas the *csrA* paralogs were genetically linked to their T4SSs, the same relationship did not exist between *csrA* paralogs and associated cargo regions (data not shown). The linkage of particular groups of *csrA* paralogs with specific T4SS lineages suggests that selective pressure(s) minimizes genetic drift between each *csrA* paralog and its associated T4SS locus. Accordingly, we investigated the functional relationship between ICE *csrA* regulators and their corresponding conjugation machinery.

Ectopic expression of *csrA* paralogs inhibits ICE transfer. ICE conjugation is mediated by its T4SS (26, 44), and the ICE-encoded T4SS loci are genetically linked to an adjacent *csrA* allele (Fig. 1). Therefore, we tested whether CsrA proteins regulate ICE transfer. ICE-βox of *L. pneumophila* Philadelphia-1 carries the *csrA* paralog *lpg2094*, which we name here *csrT* (csrA paralog for ICE transfer) (4). To test the effect of *csrT* on ICE-βox conjugative transfer, we applied both loss- and gain-of-function approaches. First, we constructed a Δ*csrT*::Gm^r deletion mutant allele and a plasmid (pcsrT) on which *csrT* transcription can be induced by IPTG. To create donor strains, we transferred either the mutant Δ*csrT* allele or pcsrT into MB1353, a derivative of the virulent Philadelphia-1 lab strain Lp02 that contains ICE-βox that has been marked with a Cam resistance cassette (4). Donor cells cultured with or without IPTG were mated with the recipient strain JR32, a lab derivative of Philadelphia-1 that does not contain ICE-βox (4).

In rich media at 37°C, deletion of *csrT* had no effect on conjugative transfer of ICE-βox (Fig. 2). On the other hand, ectopic expression of *csrT* reduced transconjugation efficiency ~10-fold. IPTG treatment did not affect transfer of ICE-βox in a strain that did not contain a *csrT* expression vector, indicating that *csrT* expression itself inhibits ICE-βox transfer.

Next, we tested whether or not the observed repression of ICE-βox conjugation by ectopic expression of its cognate *csr* gene was allele specific. Ectopic expression of *csrT* also repressed conjugation of the ICE LpgGI-1 (41) whose T4SS is from the distinct LGI lineage (Fig. 1, group IV; Fig. 2). Likewise, ectopic expression of the *csrA* paralog associated with ICE LpgGI-1 (*lpg1003*; annotated in the *L. pneumophila* Philadelphia-1 genome as *csrA-22*), reduced conjugation not only of its cognate ICE LpgGI-1 but also of ICE-βox by approximately the same amount (~10-fold reduction, Fig. 2). These data indicate that, when their expression is induced experimentally, the CsrA paralogs encoded on ICE-βox and ICE LpgGI-1 are promiscuous repressors of ICE conjugation.

ICE-βox excision is not sensitive to ectopic *csrT* expression. Conjugative transfer requires that ICEs first direct their own excision from the host chromosome (45). Because ectopic *csrT* expression reduces ICE-βox conjugation (Fig. 2) and the *lvrRABC* locus inhibits excision of it ICE Trb-1 (26), we tested whether *csrT* expression also represses ICE-βox excision. To quantify excised and integrated copies of ICE-βox, quantitative PCR using specific primers was performed as described previously (4) using template DNA isolated from donor cells cultured at 37°C in rich medium to E and PE growth phases, with or without ITPG. ICE-βox excision was not affected by ectopic expression of *csrT* in either growth phase (data not shown). Therefore, in the laboratory conditions tested, ectopic expression of *csrT* represses conjugation at some step downstream of ICE-βox excision.

Ectopic *csrT* expression represses *L. pneumophila* resistance to hydrogen peroxide conferred by ICE-βox. As another gauge of *csrA* paralog activity, we investigated whether either loss or ectopic expression of *csrT* modulates phenotypes conferred by ICE-βox. In *L. pneumophila*, ICE-βox enhances resistance to β-lactam antibiotics and oxidative stress, such as oxacillin and hydrogen peroxide (4). Therefore, we compared the capacity of ICE-βox to increase resistance to hydrogen peroxide when *L. pneumophila* either lacked or ectopically expressed *csrT*. Deletion of *csrT* did not affect bacterial survival; however, ectopic expression of WT *csrT* abrogated the capacity of ICE-βox to protect *L. pneumophila* from a 1 h exposure to 2 mM hydrogen peroxide (Fig. 3). In particular, ICE-βox$^+$ donor and transconjugant strains induced to express *csrT* were ~10-fold more susceptible to killing by hydrogen peroxide compared to the same strains cultured without IPTG induction of *csrT*. Ectopically expressed *csrT* reduced *L. pneumophila* survival by a mechanism that requires oxidative stress, since the yield of untreated strains was similar whether or not expression of pcsrT was induced with IPTG (Fig. 3). Thus, when expressed ectopically, *csrT* inhibits *L. pneumophila* resistance to hydrogen peroxide that is mediated by ICE-βox.

Ectopic *csrT* expression represses *L. pneumophila* evasion of degradative lysosomes. In addition to hydrogen peroxide, ICE-βox increases *L. pneumophila* protection from degradative lysosomes in restrictive C57BL/6 mouse macrophages (4). Therefore, as an independent measure of the capacity of *csrT* to regulate ICE-βox-mediated traits, we analyzed bacterial fate in macrophages, another source of oxidative stress (46). Because ectopic expression but not mutation of *csrT* affected hydrogen peroxide resistance (Fig. 3), the Δ*csrT* mutant strain was not included in this assay. Strains that encode or lack ICE-βox and carry pcsrT were cocultured with permissive bone marrow-derived A/J mouse macrophages in the presence or absence of IPTG. After a 90-min infection, bacterial resistance to degradation was quantified by fluorescence microscopy.

When cultured in the absence of IPTG, >80% of the ICE-βox$^+$ donor and transconjugant bacteria resisted degradation, similar to the ICE-βox$^+$ PE-phase WT Lp02 control (Fig. 4A). However, when these same strains were induced to express *csrT*, the bacteria were degraded ca. 4 to 5 times more frequently (Fig. 4A), as evidenced by particulate *L. pneumophila* antigen scattered throughout the macrophage, similar to E-phase WT Lp02 (19) and ICE-βox$^-$ JR32 cells (4). The impact of *csrT* ectopic expression appeared to be mediated by ICE-βox, since IPTG treatment of

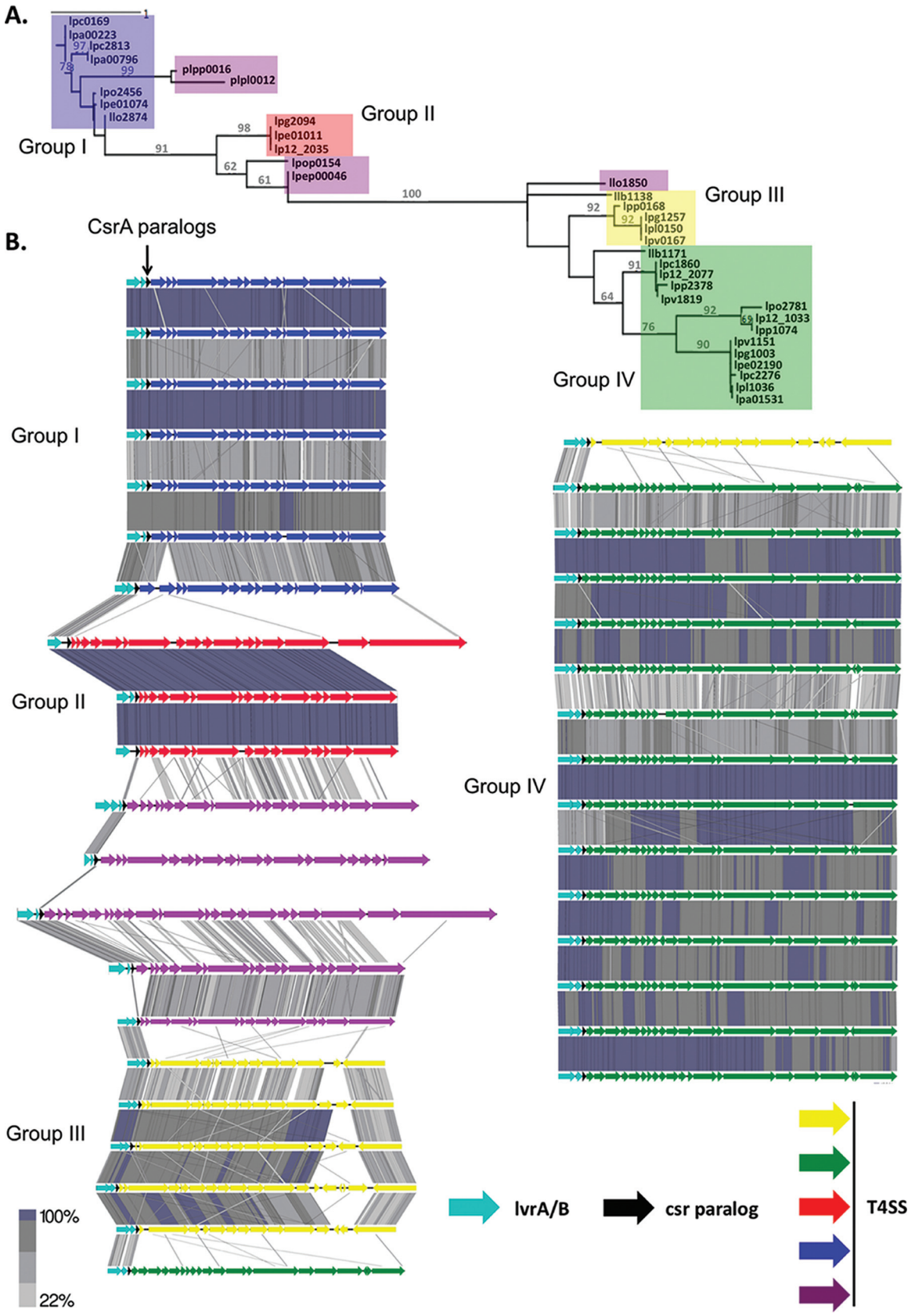
A.
lpc0169
lpa00223
lpc2813
lpa00796
lpo2456
lpe01074
llo2874
lpp0016
lpl0012
lpg2094
lpe01011
lp12_2035
lpop0154
lpep00046
llo1850
llb1138
lpp0168
lpg1257
lpl0150
lpv0167
llb1171
lpc1860
lp12_2077
lpp2378
lpv1819
lpo2781
lp12_1033
lpp1074
lpv1151
lpg1003
lpe02190
lpc2276
lpl1036
lpa01531
Group I
Group II
Group III
Group IV
B.
CsrA paralogs
Group I
Group II
Group III
Group IV
100%
22%
lvrA/B
csr paralog
T4SS

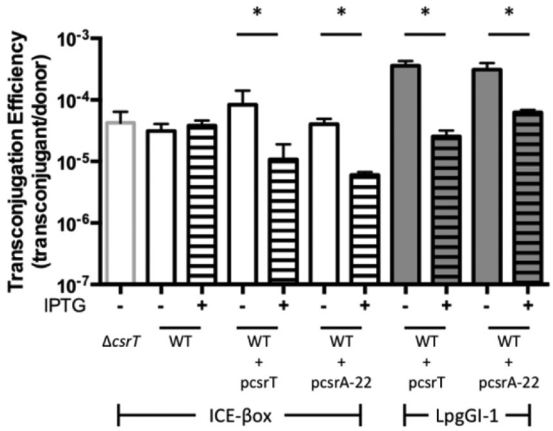

FIG 2 Ectopic *csrA paralog* expression reduces ICE transfer. The ICE-βox-null recipient strain (MB370) was mated with the following ICE-βox$^+$ donor strains (white bars): Δ*csrT* strain (MB1507), WT with no *csr* plasmid (MB1353), WT with pcsrT (MB1465), and WT with pcsrA-22 (MB1499). MB370 was also mated with the following LpgGI-1$^+$ donor strains (gray bars): WT with pcsrT (MB1500) and WT with pcsrA-22 (MB1501). The strains were cultured prior to mating without (−) or with (+) IPTG to induce ectopic expression of CsrT. Mean transconjugation efficiency of the ICEs is expressed as ($CFU_{transconjugants}/CFU_{donor}$) ± the SEM of results from one representative of two independent experiments performed at least in duplicate. A Student *t* test was used to show whether the difference between uninduced and induced transconjugation efficiency was statistically significant (*, $P < 0.05$).

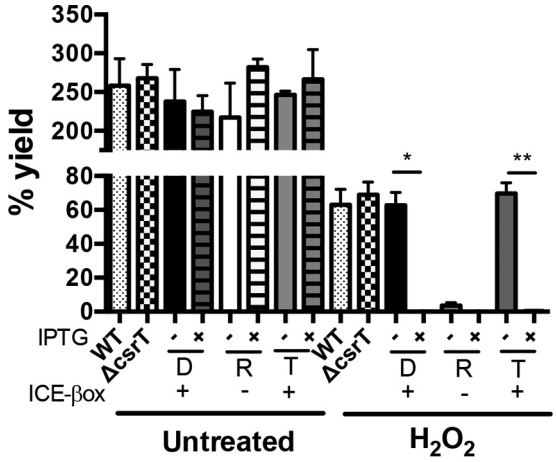

FIG 3 Ectopic *csrT* expression represses hydrogen peroxide resistance conferred by ICE-βox. CsrT abrogates the capacity of ICE-βox to protect *L. pneumophila* from hydrogen peroxide. E-phase cultures of WT Lp02 (WT, MB110), Δ*csrT* mutant (MB1409), ICE-βox$^+$ donor (D), ICE-βox$^-$ recipient (R), and ICE-βox$^+$ transconjugant (T) strains that contained IPTG-inducible plasmid pcsrT (strains MB1383, MB1384, and MB1385, respectively) were cultured overnight without (−) or with (+) IPTG and then exposed to 2 mM H_2O_2 for 1 h. The mean percent survival ± the SEM was calculated from three independent experiments as ($CFU_{posttreatment}/CFU_{pretreatment}$) × 100. Student *t* tests were used to determine statistically significant differences between treated, pcsrT-induced ICE-βox$^+$ strains and treated uninduced strains (*, $P < 0.05$; **, $P < 0.01$). Note that after induction of pcsrT expression, the yields of D, R, and T strains were <1%, values that are not visible on this scale.

bacteria that carried pcsrT but lacked ICE-βox did not measurably increase bacterial degradation.

As expected, when *csrT* was ectopically expressed by strains that carried ICE-βox, we also observed a modest but reproducible and statistically significant increase in colocalization of the late endosomal and lysosomal marker LAMP-1 with the intracellular bacteria (Fig. 4B) (35, 47). Again, ectopic expression had no appreciable effect on the isogenic strain that did not encode ICE-βox (Fig. 4B).

To verify our microscopic assays of bacterial fate in macrophages (Fig. 4A and B), we quantified the viability of cell-associated *L. pneumophila*. Permissive bone marrow-derived A/J mouse macrophages were infected with strains that carry pcsrT and encode or lack ICE-βox after culture with or without IPTG. After a 90-min infection, the fraction of input bacteria that were viable and cell associated was quantified. Consistent with our microscopy data, ectopic expression of *csrT* markedly reduced the cell-associated CFU for ICE-βox$^+$ donor and transconjugant cultures (Fig. 4C). Therefore, ectopic expression of *csrT* is sufficient to inhibit two traits conferred by ICE-βox: resistance to hydrogen peroxide and to degradation in macrophages.

In addition, we noted that induction of pcsrT modestly decreased the already poor infectivity of the ICE-βox-negative recipient strain (Fig. 4C) ($P < 0.05$). This observation raised the possibility that, in addition to repressing ICE-βox-encoded traits (Fig. 3 and 4), ectopic *csrT* expression also affects components of the *L. pneumophila* core genome.

Ectopic *csrT* expression inhibits *L. pneumophila* growth in macrophages that encode or lack NADPH oxidase. *L. pneumophila* containing the ICE-βox replicates more efficiently in macrophages than do bacteria that lack the element (4). Because ectopic expression of *csrT* represses ICE-βox-mediated oxidative stress resistance in broth (Fig. 3) and survival in macrophages (Fig. 4), we predicted *csrT* would also inhibit intracellular growth of *L. pneumophila*. To test the impact of *csrT* on intracellular replication, bone marrow-derived A/J mouse macrophages were infected with ICE-βox$^+$ *L. pneumophila* carrying pcsrT and cultured with or without IPTG. After 48 h, bacterial yield was quantified and expressed as the fold increase relative to the number of intracellular bacteria present at 2 h, a method that accounts for differences in infectivity (Fig. 4C). Consistent with their poor survival of oxidative stress (Fig. 3) and macrophage infection (Fig. 4), after 48 h of coculture, bacteria that ectopically expressed *csrT* were recovered at a significantly reduced yield (~100-fold, $P < 0.005$) (Fig. 5A).

In macrophages, ICE-βox protects *L. pneumophila* from oxidative stress generated by the NADPH oxidase (4). Therefore, to test the contribution of the phagocyte oxidase to the poor yield of

FIG 1 Relationship of CsrA paralogs and T4SSs. (A) To determine the relationship between 34 ICE-associated *csrA* loci, a maximum-likelihood phylogenetic tree was generated from their predicted amino acid sequences. Four distinct clusters are boxed in blue (group 1, Trb), red (group II, Tra), yellow (group III, Lvh), and green (group IV, Lgi). The five protein sequences that did not clearly fall into any cluster are boxed in purple. Branches with at least 60% support from 100 bootstraps are labeled. (B) Pairwise translated nucleotide sequence identity (tBLASTx) of 34 T4SSs in the legionella pangenome was performed based on the relationship of their adjacent *csrA* paralogs as determined by the phylogeny in panel A. *lvrA/B* genes are teal arrows; *csrA* paralogs are black arrows and indicated by a pointer; T4SSs are colored and labeled by group to correspond with the boxes in panel A. Gray bars between T4SS operons indicate the percent identity as shown by the scale bar. For continuity, the bottom two T4SSs from the left column are reproduced as the top two in the right column.

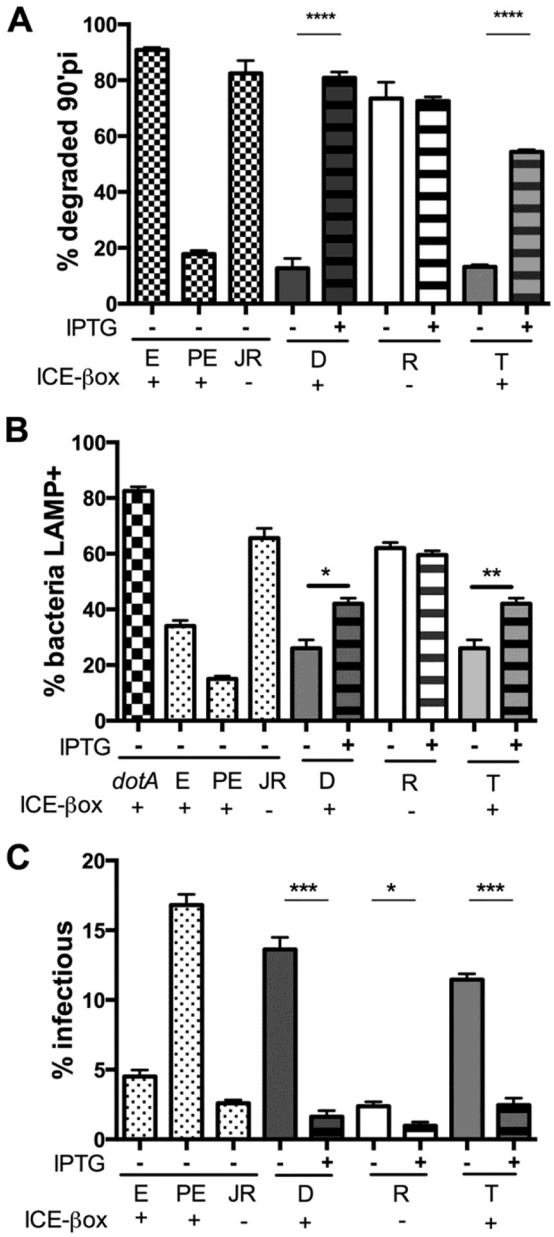

FIG 4 Ectopic *csrT* expression reduces *L. pneumophila* infection of macrophages. (A) CsrT induction increases *L. pneumophila* degradation in macrophages. E- and PE-phase strain ICE-βox$^+$ Lp02 (MB110) and PE-phase ICE-βox null strain JR32 (JR; MB370) (hatched bars); ICE-βox donor (D), recipient (R), or transconjugant (T) strains containing the inducible pcsrT plasmid (MB1383, MB1384, and MB1385, respectively) were cultured overnight without (−) or with (+) IPTG and then incubated for 90 min with A/J macrophages at an MOI of 2 (induced) or 1 (uninduced). After fixation, bacterial integrity was quantified by immunofluorescence microscopy. Presented are the mean percents ± the SEM of total bacteria that were degraded from three independent experiments. Student *t* tests were used to determine that differences between induced and uninduced D and T strains are significant ($P < 0.001$). (B) Ectopic *csrT* expression increases *L. pneumophila* trafficking to LAMP-1$^+$ compartments. Bacteria were cultured and macrophages were infected as for panel A, and then macrophages were stained with antibodies specific to *Legionella* and LAMP-1. Colocalization of *L. pneumophila* with LAMP-1 was quantified by immunofluorescence microscopy. Presented are the mean percents ± the SEM of *L. pneumophila* that colocalized with LAMP-1 determined from three coverslips in one experiment that is representative of three independent experiments. Student *t* tests were used to determine that differences between induced and uninduced ICE-βox$^+$ D and T strains are significant (*, $P < 0.05$; **, $P < 0.01$). A Δ*dotA* mutant was included as a positive control for LAMP-1$^+$ staining. (C) CsrT induction inhibits *L. pneumophila* infection of macrophages. A/J mouse macrophages were infected as described for panel A. After a 90-min infection, cells were lysed and CFU were enumerated. The percent infectious bacteria was calculated as (CFU at 90 min/CFU of input) × 100 and is expressed as the mean ± the SEM from three replicates in one experiment representative of three others. A Student *t* test was used to confirm whether differences between induced and uninduced strains are significant (*, $P < 0.05$; ***, $P < 0.005$).

strains induced to express *csrT*, J774.16 WT and J774.D9 NADPH oxidase mutant macrophage cells were infected with ICE-βox$^+$ strains carrying pcsrT and cultured with or without IPTG; after 48 h, the yield of intracellular bacteria was quantified. Much like the A/J mouse macrophage infection (Fig. 5A), the bacterial yield from J774.16 WT macrophages was significantly reduced by ectopic expression of *csrT* (~80-fold less, $P < 0.005$, Fig. 5B). In addition, *csrT* expression reduced the yield of *L. pneumophila* in the J774.D9 NADPH oxidase mutants, although to a lesser extent (~50-fold less, $P < 0.005$, Fig. 5C). Therefore, ectopic expression of *csrT* also inhibits *L. pneumophila* infection in macrophages by a mechanism(s) not solely dependent on either the macrophage NADPH oxidase (Fig. 5C) or ICE-βox (Fig. 4C).

Ectopic *csrT* expression inhibits motility and flagellar assembly in *L. pneumophila*. Maximal infection of macrophages by *L. pneumophila* requires evasion of the macrophage oxidative burst and endosomal pathway (35, 48), as well as bacterial motility, which increases contacts with host phagocytes (49). Canonical CsrA represses not only Dot/Icm T4SS activity but also motility (19, 20, 50), establishing a precedent that *L. pneumophila* motility and T4SSs can belong to the same regulon. Therefore, we investigated whether *csrT* expression represses motility, a broadly conserved trait encoded by the core genome. Indeed, when PE-phase *L. pneumophila* ectopically expressed *csrT*, only ~ 5% of the bacteria were motile, compared to ca. 90% of uninduced control cells, as judged by phase microscopy (Fig. 6A). Repression of flagellin expression and motility by ectopically expressed *csrT* could not be accounted for by a general inhibition of *L. pneumophila* differentiation into the transmissive phase, since IPTG treatment of strains carrying pcsrT did not inhibit expression of other PE traits, including cell shortening, pigment production, and sodium sensitivity (data not shown).

To probe the mechanism of *csrT* inhibition of motility, we analyzed flagellin levels by Western analysis of *L. pneumophila* cultured with or without induced *csrT* expression. As a positive control, we induced ectopic expression of canonical *csrA*, a known repressor of the *L. pneumophila* flagellar operon (19, 20, 43). Similar to *csrA*, induction of *csrT* decreased flagellin protein levels (Fig. 6A). The observation that ectopic expression of either *csrA* or *csrT* inhibits flagellin production is consistent with the hypothesis that the family of ICE-associated *csrA* loci (Fig. 1) retain function as regulatory proteins.

***csrT* inhibits motility in *B. subtilis* via a conserved RNA-binding mechanism.** As in *L. pneumophila*, the *B. subtilis* CsrA protein inhibits bacterial motility (51). Because the CsrA-binding site on a specific mRNA target, *hag*, is defined in *B. subtilis*, we utilized this system to investigate whether CsrT of *L. pneumophila* ICE-βox can also regulate gene expression by binding mRNA. In particular, we exploited two *B. subtilis* mutants: the Δ*fliW sow3* mutant, which is insensitive to CsrA repression of motility due to

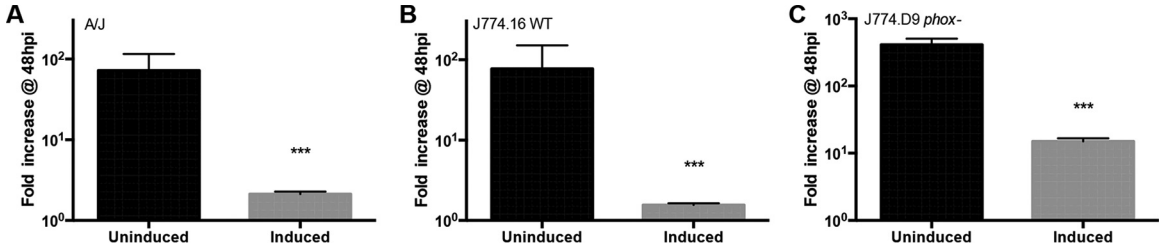

FIG 5 Ectopic *csrT* expression reduces *L. pneumophila* yield in macrophages that encode or lack NADPH oxidase. A/J mouse macrophages (A), J774.16 WT macrophage cells (B), and J774.D9 *phox* mutant macrophage cells (C) were infected with ICE-βox$^+$ WT Lp02 carrying pcsrT (MB1383) that had been cultured overnight without or with IPTG induction at an MOI of 1 (uninduced) or 2 (induced). The results are expressed as the fold increase in CFU at 48 h postinfection (hpi) relative to the 2-h time point (CFU at 48 hpi/CFU at 2 hpi). Shown are means ± the SEM from one experiment that is representative of three others. In all macrophage backgrounds, Student *t* tests were used to confirm whether the differences in bacterial yield for uninduced and induced strains are significant ($P < 0.005$).

a point mutation in its CsrA binding site on the *hag* mRNA, which encodes flagellin, and the Δ*fliW* mutant, which lacks the protein that binds and antagonizes the CsrA repressor protein (51). Swarming motility by *B. subtilis* WT and Δ*fliW sow3* mutant strains that ectopically expressed *csrA* paralogs of *B. subtilis* or *L. pneumophila* was quantified.

Induction of either *B. subtilis csrA* or *L. pneumophila csrT* inhibited motility in WT *B. subtilis* (Fig. 6C and D). Moreover, the mechanism of repression was specific, since neither *B. subtilis csrA* nor *L. pneumophila csrT* inhibited motility in the Δ*fliW sow3* mutant, which lacks the mRNA binding site for the *B. subtilis* CsrA repressor (51) (Fig. 6C and D). Since a single point mutation in the

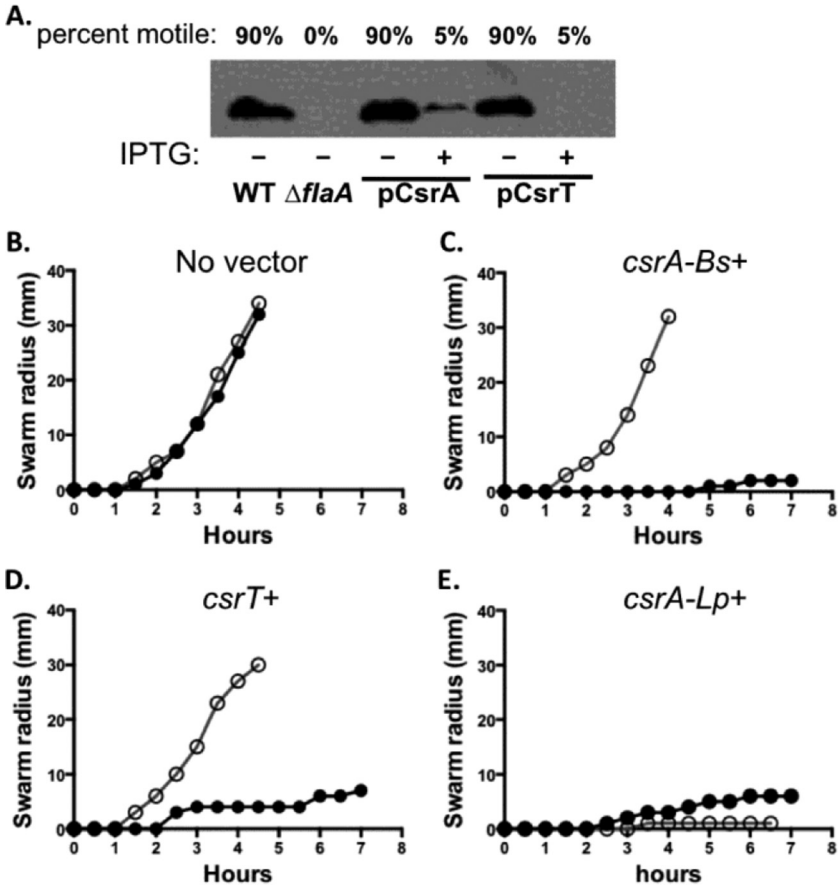

FIG 6 Ectopic *csrT* expression inhibits motility via a conserved mechanism. (A) Western analysis of flagellin protein was performed on PE-phase cultures of *L. pneumophila* strain Lp02 carrying pcsrA (MB1389) or pcsrT (MB1383), induced (+) or not induced (−) with IPTG as indicated. Lp02 WT with no vector (MB110) was used as a positive control, and a *flaA* mutant (MB1390) was used as a negative control. The percentage of bacteria that were motile was judged by phase microscopy of wet mounts. Shown are results of one experiment that is representative of at least three others. (B to E) *B. subtilis* swarming motility was assessed on swarm agar plates every 30 min for WT (filled circles; strain 3610) and *fliW sow3* mutants, which are insensitive to *B. subtilis* CsrA repression mutant (open circles; DS6530) with no vector (B), induced expression of *B. subtilis csrA* (DS4940 and DK1469) (C), induced expression of *L. pneumophila csrT* (DK677 and DK1471) (D), or induced expression of *L. pneumophila csrA* (DK675 and DK1470) (E). Plots represent the means of triplicate plates from one experiment.

hag mRNA was sufficient to abrogate CsrT repression of motility, this CsrA paralog encoded by ICE-βox likely binds to *hag* mRNA and inhibits its translation. Therefore, both bioinformatic (22) and genetic data (Fig. 2 to 6) are consistent with the model that CsrT functions as an RNA binding protein that regulates gene expression.

Like *B. subtilis csrA* and ICE-βox *csrT*, induction of canonical *csrA* of *L. pneumophila* also inhibited *B. subtilis* swarming (Fig. 6E). However, *L. pneumophila csrA* did so even when the *hag* mRNA binding site was mutated (Fig. 6E). Therefore, although the canonical CsrA repressor encoded by the core *L. pneumophila* genome does bind mRNA (22), its sequence specificity may be different from that of *B. subtilis* CsrA and *L. pneumophila* ICE-βox CsrT.

DISCUSSION

Legionellae must adapt to assault from diverse environmental and intracellular stresses, and horizontally acquired ICEs may increase the fitness of this opportunistic pathogen (4, 23–25, 52, 53). We demonstrate here that every *L. pneumophila* ICE identified to date encodes a *csrA*-like locus that is genetically linked to a particular T4SS lineage (Fig. 1; see Table S2 in the supplemental material). The *csrA* paralog encoded by *L. pneumophila* ICE-βox retains regulatory potential, as judged by the capacity of ectopically expressed *csrT* to repress not only conjugative transfer and oxidative stress resistance encoded by its cognate mobile element (Fig. 2 and 3) but also conjugation of a distinct lineage of ICE (group IV LpgGI-1) (Fig. 1 and 2), as well as *L. pneumophila* infection of macrophages (Fig. 4 and 5) and flagellin expression (Fig. 6A) and *B. subtilis* swarming motility (Fig. 6B to E).

By exploiting the well-characterized *B. subtilis* swarming motility pathway, we demonstrate that CsrT likely functions by binding mRNA (Fig. 6D). Since a point mutation of the CsrA binding site on the *B. subtilis* target mRNA was sufficient to relieve repression by ectopically expressed ICE-βox *csrT*, we deduce that CsrT protein binds mRNA by specifically recognizing the ANGGA consensus sequence for CsrA binding that several bacterial species use (51, 54–56). Indeed, the CsrT protein has retained many of the key residues that equip *E. coli* CsrA to bind mRNA (22, 57). Together, our bioinformatic, genetic and functional analyses indicate that CsrT is an RNA binding protein capable of regulating gene expression. Future biochemical experiments can verify that CsrT protein directly interacts with mRNA and identify its specific targets in *L. pneumophila*.

We favor the model developed for *B. subtilis* that CsrA proteins regulate nanomachineries (51) and speculate that the CsrA paralog encoded on each *L. pneumophila* ICE regulates its cognate T4SS machinery. *B. subtilis* controls flagella morphogenesis by a partner-switching mechanism comprised of the FliW regulator, a CsrA repressor, and flagellin (*hag*) subunits (51). It is striking that, just as *fliW*, *csrA*, and *hag* are encoded in tandem on the *B. subtilis* chromosome, every known *L. pneumophila* ICE carries a similar gene trio that encodes a putative regulatory protein (LvrA/B), a CsrA repressor, and a pilin structural protein (Fig. 1B). Accordingly, the hypothesis that, under physiological conditions, CsrT regulates assembly of the ICE-βox T4SS apparatus and CsrA-22 controls ICE LpgGI-1 warrants direct testing.

Although our conjugation experiments suggest that the *csrA* paralogs may retain some overlapping activity (Fig. 2), gene duplication events and subsequent genetic drift appear to have diversified the *L. pneumophila* family of core and ICE-associated *csrA* genes (22) (Fig. 1; see Table S2 in the supplemental material). For example, canonical CsrA represses expression of *csrR* by binding to its mRNA at an ANGGA motif that overlaps the start codon (22). Likewise, an ANGGA binding site on the *hag* RNA is required for CsrT of ICE-βox to repress *B. subtilis* motility (Fig. 6). However, canonical CsrA represses *B. subtilis* motility despite a point mutation in the ANGAA motif (Fig. 6), indicating divergence between these two *L. pneumophila* paralogs. Instead, canonical *csrA* is predicted to bind AGGA motifs in the mRNAs of multiple substrates of the *dot/icm* T4SS to regulate their expression; among this class of targets, ANGGA motifs are more rare (19, 20). Differences among the *L. pneumophila csrA* paralogs were also revealed by our phenotypic analysis. *L. pneumophila* motility is inhibited by ectopic expression of *csrT* (Fig. 6A) but not of *csrA-22* or another ICE-associated *csrA* paralog, *lpg1257* of ICE-Trb-1, both of whose protein sequences are less similar to canonical CsrA. Likewise, *B. subtilis* motility is inhibited by ectopic expression of three of the *csrA* paralogs encoded by *L. pneumophila* strain Lp02 (core *csrA*, ICE-βox *csrT*, and *lpg1257*) but not two others (core *csrR* and *csrA-22* [22]) (see Table S2 in the supplemental material; also data not shown). Therefore, we speculate that genetic drift of individual ICE *csrA* paralogs may accommodate distinct regulatory demands of their corresponding T4SS class (Fig. 1), concomitantly relaxing their capacity to repress motility of their bacterial host.

Our bioinformatics analysis also predicts that some RNA targets of CsrT are encoded within its associated T4SS locus. Sequence alignment of 34 ICE-associated *csrA* paralogs revealed at least four distinct *csrA* gene families and CsrA-T4SS pairs (Fig. 1; see Table S2 in the supplemental material). The high degree of similarity within each of the four distinct *csrA* groups indicates that the ICE-encoded *csrA* loci are under selective pressure to maintain function. Moreover, the genetic linkage of each *csrA* paralog group to one of four previously identified T4SS lineages (Fig. 1B)—Tra (4), LGI (41), Trb (42), and Lvh (43)—predicts a functional relationship between ICE *csrA* paralogs and T4SSs. Whereas the specific amino acid sequence of each *csrA* paralog appears to be genetically constrained by the composition of the adjacent T4SS locus (Fig. 1), the same cannot be said for the associated cargo regions, which are diverse (data not shown). Therefore, we favor the model that CsrT of ICE-βox regulates its associated T4SS, rather than expression of ICE cargo genes.

It is possible that all—or at least some—of the ICE-associated CsrA paralogs are capable of promiscuous interaction with mRNAs encoding multiple T4SSs or traits encoded in the core genome. When ectopically expressed, either *csrT* or *csrA-22* (*lpg1003*) reduced transfer of ICE-βox or ICE-LpgGI-1 by ~10-fold (Fig. 2), and *csrT* and *csrA-22* (*lpg1003*) are members of distinct lineages (group IV and group II, respectively) (Fig. 1). In addition, when expressed ectopically, *csrT* slightly reduced the infectivity of *L. pneumophila* that lacked ICE-βox (Fig. 4C). Induced *csrT* expression also reduced the bacterial yield in the J774.D9 phagocyte oxidase mutant cell line (Fig. 5C), even though these cells are permissive for growth of *L. pneumophila* that do not encode ICE-βox (4). Furthermore, CsrT inhibits *L. pneumophila* flagellin expression and motility (Fig. 6A), a broadly conserved trait that contributes to virulence (19). The reduced motility of cultures that ectopically express *csrT* likely contributes to their poor infectivity (Fig. 4C), since amotile *L. pneumophila* are less

infectious in cell culture due to decreased contacts with macrophages (49). Inhibition of flagellin production by ectopically expressed CsrT may simply reflect its ancestry as a homologue of canonical CsrA, a repressor of *L. pneumophila* motility (19). It is also formally possible that the capacity of CsrT to repress motility increases fitness of ICE-βox, since bacteria conjugate more efficiently when stationary.

However, a limitation of our phenotypic analyses is the reliance on ectopic expression of *csrA* paralogs (Fig. 2 to 6), rather than loss of function. In rich medium at 37°C, excision of ICE-βox, expression of its T4SS genes, and the conjugation efficiency are quite low (data not shown and Fig. 2). If *csrT* is not naturally expressed under the conditions tested, deletion of *csrT* would have no observable phenotype. Ectopic expression bypasses the need to know a gene's natural inducers or regulatory circuit; nevertheless, it is a blunt genetic tool. For example, ectopic expression is likely to confound the nuances of local concentrations of protein and RNA in the bacterial cell that are known to be important for CsrA protein interaction with its RNA targets. CsrA proteins have different affinities for mRNA targets based on sequence of the RNA binding site and side chains of the CsrA protein (54, 56). The local concentration of protein and RNA therefore dictate whether high- or low-affinity interactions occur. Indeed, local concentrations of mRNAs are not constant in the intracellular space of bacteria (58). Moreover, CsrA proteins function as dimers and can also form complexes with other regulatory proteins (51, 54). Therefore, induced expression of *csrA* paralogs from a multicopy vector may enable protein-RNA or protein-protein interactions that do not occur in nature. Accordingly, at present we can definitively conclude only that *csrT* has the capacity to inhibit multiple traits encoded by ICE-βox and the core genome. Identifying laboratory conditions that are optimal for *csrT* expression and the bona fide targets of CsrT regulation is a goal of future work.

Using bioinformatic analysis (Fig. 1) (22), we describe a new large class of *csrA*-like genes associated with T4SSs in ICEs never before characterized in *Legionella* or any other bacterial genus. The genetic linkage of these paralogs with T4SSs strongly predicts a functional relationship between the two. Furthermore, the observation that ectopic expression of *csrT* inhibits phenotypes as diverse as ICE conjugation and *L. pneumophila* and *B. subtilis* motility not only demonstrates that CsrT is a functional paralog of CsrA but also raises intriguing questions as to why *csrA* regulators are ubiquitous among *L. pneumophila* ICEs. By analogy to *B. subtilis*' partner-switching mechanism that regulates flagellum morphogenesis (51), we postulate that the assembly of ICE T4SS pili are governed by interactions between LvrA/B, CsrA, and pilin proteins. It is also noteworthy that, in *L. pneumophila*, CsrA is an essential pluripotent posttranscriptional repressor of transmission traits that the intracellular pathogen requires to replicate *in vitro* and in macrophages and amoebae (19, 20). Moreover, CsrA directly binds and represses translation of *csrR* mRNA, which encodes a second broadly conserved core *csrA* paralog that enhances *L. pneumophila* survival in water (22). Accordingly, it is feasible that some ICE *csrA* paralogs increase the fitness of their mobile elements by retaining the capacity to manipulate core life cycle switches of its host bacterium. In either case, a posttranscriptional regulator would equip the ICE to load its host cell with a pool of transcripts whose translation can be quickly derepressed when environmental conditions favor T4SS assembly and ICE spread. Thus, we postulate that conserved *csrA*-like regulators equip *Legionella* ICEs to coordinate expression of traits that ensure their maintenance within bacterial populations.

ACKNOWLEDGMENTS

We thank Paul Carlson for technical guidance, Phil Hanna's lab for the use of equipment, and Renee Tsolis for the J774 cell lines.

This study was supported by the Endowment for the Basic Sciences at the University of Michigan Medical School (M.S.S.), two University of Michigan Rackham Merit Fellowships (K.J.F. and Z.D.A.), the Molecular Mechanisms of Microbial Pathogenesis training program (NIH T32 AI007528; K.J.F.), the Cellular Biotechnology training program (NIH T32 GM008353; Z.D.A.), and the NIH R01 (grant GM093030 to D.B.K.).

The funders had no role in study design, data collection and interpretation, or the decision to submit the work for publication.

FUNDING INFORMATION

HHS | NIH | National Institute of Allergy and Infectious Diseases (NIAID) provided funding to Kaitlin Flynn under grant number T32 AI007528. HHS | NIH | National Institute of Allergy and Infectious Diseases (NIAID) provided funding to Zachary D. Abbott under grant number T32 GM008353. HHS | NIH | National Institute of General Medical Sciences (NIGMS) provided funding to Daniel B. Kearns under grant number GM093030.

REFERENCES

1. **Wozniak RA, Waldor MK.** 2010. Integrative and conjugative elements: mosaic mobile genetic elements enabling dynamic lateral gene flow. Nat Rev Microbiol **8:**552–563. http://dx.doi.org/10.1038/nrmicro2382.
2. **Beaber JW, Hochhut B, Waldor MK.** 2004. SOS response promotes horizontal dissemination of antibiotic resistance genes. Nature **427:**72–74. http://dx.doi.org/10.1038/nature02241.
3. **Rodriguez-Blanco A, Lemos ML, Osorio CR.** 2012. Integrating conjugative elements as vectors of antibiotic, mercury, and quaternary ammonium compound resistance in marine aquaculture environments. Antimicrob Agents Chemother **56:**2619–2626. http://dx.doi.org/10.1128/AAC.05997-11.
4. **Flynn KJ, Swanson MS.** 2014. Integrative conjugative element ICE-betaox confers oxidative stress resistance to *Legionella pneumophila in vitro* and in macrophages. mBio **5:**e01091–14. http://dx.doi.org/10.1128/mBio.01091-14.
5. **Koraimann G, Wagner MA.** 2014. Social behavior and decision making in bacterial conjugation. Front Cell Infect Microbiol **4:**54. http://dx.doi.org/10.3389/fcimb.2014.00054.
6. **Juhas M, Crook DW, Hood DW.** 2008. Type IV secretion systems: tools of bacterial horizontal gene transfer and virulence. Cell Microbiol **10:**2377–2386. http://dx.doi.org/10.1111/j.1462-5822.2008.01187.x.
7. **Frost LS, Koraimann G.** 2010. Regulation of bacterial conjugation: balancing opportunity with adversity. Future Microbiol **5:**1057–1071. http://dx.doi.org/10.2217/fmb.10.70.
8. **Stone BJ, Abu Kwaik Y.** 1998. Expression of multiple pili by *Legionella pneumophila*: identification and characterization of a type IV pilin gene and its role in adherence to mammalian and protozoan cells. Infect Immun **66:**1768–1775.
9. **Segal G, Shuman HA.** 1998. Intracellular multiplication and human macrophage killing by *Legionella pneumophila* are inhibited by conjugal components of IncQ plasmid RSF1010. Mol Microbiol **30:**197–208. http://dx.doi.org/10.1046/j.1365-2958.1998.01054.x.
10. **Bose B, Auchtung JM, Lee CA, Grossman AD.** 2008. A conserved anti-repressor controls horizontal gene transfer by proteolysis. Mol Microbiol **70:**570–582. http://dx.doi.org/10.1111/j.1365-2958.2008.06414.x.
11. **Sentchilo V, Ravatn R, Werlen C, Zehnder AJ, van der Meer JR.** 2003. Unusual integrase gene expression on the clc genomic island in Pseudomonas sp. strain B13. J Bacteriol **185:**4530–4538. http://dx.doi.org/10.1128/JB.185.15.4530-4538.2003.
12. **Wang Y, Shoemaker NB, Salyers AA.** 2004. Regulation of a Bacteroides operon that controls excision and transfer of the conjugative transposon CTnDOT. J Bacteriol **186:**2548–2557. http://dx.doi.org/10.1128/JB.186.9.2548-2557.2004.
13. **Bose B, Grossman AD.** 2011. Regulation of horizontal gene transfer in

Bacillus subtilis by activation of a conserved site-specific protease. J Bacteriol **193:**22–29. http://dx.doi.org/10.1128/JB.01143-10.
14. **Clewell DB.** 2011. Tales of conjugation and sex pheromones: A plasmid and enterococcal odyssey. Mob Genet Elements **1:**38–54. http://dx.doi.org/10.4161/mge.1.1.15409.
15. **Haudecoeur E, Faure D.** 2010. A fine control of quorum-sensing communication in *Agrobacterium tumefaciens*. Commun Integr Biol **3:**84–88. http://dx.doi.org/10.4161/cib.3.2.10429.
16. **Rao C, Benhabib H, Ensminger AW.** 2013. Phylogenetic reconstruction of the *Legionella pneumophila* Philadelphia-1 laboratory strains through comparative genomics. PLoS One **8:**e64129. http://dx.doi.org/10.1371/journal.pone.0064129.
17. **Chien M, Morozova I, Shi S, Sheng H, Chen J, Gomez SM, Asamani G, Hill K, Nuara J, Feder M, Rineer J, Greenberg JJ, Steshenko V, Park SH, Zhao B, Teplitskaya E, Edwards JR, Pampou S, Georghiou A, Chou IC, Iannuccilli W, Ulz ME, Kim DH, Geringer-Sameth A, Goldsberry C, Morozov P, Fischer SG, Segal G, Qu X, Rzhetsky A, Zhang P, Cayanis E, De Jong PJ, Ju J, Kalachikov S, Shuman HA, Russo JJ.** 2004. The genomic sequence of the accidental pathogen *Legionella pneumophila*. Science **305:**1966–1968. http://dx.doi.org/10.1126/science.1099776.
18. **Cazalet C, Jarraud S, Ghavi-Helm Y, Kunst F, Glaser P, Etienne J, Buchrieser C.** 2008. Multigenome analysis identifies a worldwide distributed epidemic *Legionella pneumophila* clone that emerged within a highly diverse species. Genome Res **18:**431–441. http://dx.doi.org/10.1101/gr.7229808.
19. **Molofsky AB, Swanson MS.** 2003. *Legionella pneumophila* CsrA is a pivotal repressor of transmission traits and activator of replication. Mol Microbiol **50:**445–461. http://dx.doi.org/10.1046/j.1365-2958.2003.03706.x.
20. **Nevo O, Zusman T, Rasis M, Lifshitz Z, Segal G.** 2014. Identification of *Legionella pneumophila* effectors regulated by the LetAS-RsmYZ-CsrA regulatory cascade, many of which modulate vesicular trafficking. J Bacteriol **196:**681–692. http://dx.doi.org/10.1128/JB.01175-13.
21. **Marden JN, Diaz MR, Walton WG, Gode CJ, Betts L, Urbanowski ML, Redinbo MR, Yahr TL, Wolfgang MC.** 2013. An unusual CsrA family member operates in series with RsmA to amplify posttranscriptional responses in *Pseudomonas aeruginosa*. Proc Natl Acad Sci U S A **110:**15055–15060. http://dx.doi.org/10.1073/pnas.1307217110.
22. **Abbott ZD, Yakhnin H, Babitzke P, Swanson MS.** 2015. *csrR*, a paralog and direct target of CsrA, promotes *Legionella pneumophila* resilience in water. mBio **6:**e00595. http://dx.doi.org/10.1128/mBio.00595-15.
23. **O'Connor TJ, Adepoju Y, Boyd D, Isberg RR.** 2011. Minimization of the *Legionella pneumophila* genome reveals chromosomal regions involved in host range expansion. Proc Natl Acad Sci U S A **108:**14733–14740. http://dx.doi.org/10.1073/pnas.1111678108.
24. **Cazalet C, Rusniok C, Bruggemann H, Zidane N, Magnier A, Ma L, Tichit M, Jarraud S, Bouchier C, Vandenesch F, Kunst F, Etienne J, Glaser P, Buchrieser C.** 2004. Evidence in the *Legionella pneumophila* genome for exploitation of host cell functions and high genome plasticity. Nat Genet **36:**1165–1173. http://dx.doi.org/10.1038/ng1447.
25. **Gomez-Valero L, Rusniok C, Jarraud S, Vacherie B, Rouy Z, Barbe V, Medigue C, Etienne J, Buchrieser C.** 2011. Extensive recombination events and horizontal gene transfer shaped the *Legionella pneumophila* genomes. BMC Genomics **12:**536. http://dx.doi.org/10.1186/1471-2164-12-536.
26. **Lautner M, Schunder E, Herrmann V, Heuner K.** 2013. Regulation, integrase-dependent excision, and horizontal transfer of genomic islands in *Legionella pneumophila*. J Bacteriol **195:**1583–1597. http://dx.doi.org/10.1128/JB.01739-12.
27. **Feeley JC, Gibson RJ, Gorman GW, Langford NC, Rasheed JK, Mackel DC, Baine WB.** 1979. Charcoal-yeast extract agar: primary isolation medium for *Legionella pneumophila*. J Clin Microbiol **10:**437–441.
28. **Larkin MA, Blackshields G, Brown NP, Chenna R, McGettigan PA, McWilliam H, Valentin F, Wallace IM, Wilm A, Lopez R, Thompson JD, Gibson TJ, Higgins DG.** 2007. Clustal W and Clustal X version 2.0. Bioinformatics **23:**2947–2948. http://dx.doi.org/10.1093/bioinformatics/btm404.
29. **Guindon S, Dufayard JF, Lefort V, Anisimova M, Hordijk W, Gascuel O.** 2010. New algorithms and methods to estimate maximum-likelihood phylogenies: assessing the performance of PhyML 3.0. Syst Biol **59:**307–321. http://dx.doi.org/10.1093/sysbio/syq010.
30. **Letunic I, Bork P.** 2011. Interactive Tree Of Life v2: online annotation and display of phylogenetic trees made easy. Nucleic Acids Res **39:**W475–W478. http://dx.doi.org/10.1093/nar/gkr201.
31. **Sullivan MJ, Petty NK, Beatson SA.** 2011. Easyfig: a genome comparison visualizer. Bioinformatics **27:**1009–1010. http://dx.doi.org/10.1093/bioinformatics/btr039.
32. **Dalebroux ZD, Yagi BF, Sahr T, Buchrieser C, Swanson MS.** 2010. Distinct roles of ppGpp and DksA in *Legionella pneumophila* differentiation. Mol Microbiol **76:**200–219. http://dx.doi.org/10.1111/j.1365-2958.2010.07094.x.
33. **Bryan A, Harada K, Swanson MS.** 2011. Efficient generation of unmarked deletions in *Legionella pneumophila*. Appl Environ Microbiol **77:**2545–2548. http://dx.doi.org/10.1128/AEM.02904-10.
34. **Swanson MS, Isberg RR.** 1995. Association of *Legionella pneumophila* with the macrophage endoplasmic reticulum. Infect Immun **63:**3609–3620.
35. **Swanson MS, Isberg RR.** 1996. Identification of *Legionella pneumophila* mutants that have aberrant intracellular fates. Infect Immun **64:**2585–2594.
36. **Goldberg M, Belkowski LS, Bloom BR.** 1990. Regulation of macrophage function by interferon-gamma. Somatic cell genetic approaches in murine macrophage cell lines to mechanisms of growth inhibition, the oxidative burst, and expression of the chronic granulomatous disease gene. J Clin Invest **85:**563–569.
37. **Vogel JP, Andrews HL, Wong SK, Isberg RR.** 1998. Conjugative transfer by the virulence system of *Legionella pneumophila*. Science **279:**873–876. http://dx.doi.org/10.1126/science.279.5352.873.
38. **Gibson DG, Young L, Chuang RY, Venter JC, Hutchison CA, III, Smith HO.** 2009. Enzymatic assembly of DNA molecules up to several hundred kilobases. Nat Methods **6:**343–345. http://dx.doi.org/10.1038/nmeth.1318.
39. **Yasbin RE, Young FE.** 1974. Transduction in *Bacillus subtilis* by bacteriophage SPP1. J Virol **14:**1343–1348.
40. **Doleans-Jordheim A, Akermi M, Ginevra C, Cazalet C, Kay E, Schneider D, Buchrieser C, Atlan D, Vandenesch F, Etienne J, Jarraud S.** 2006. Growth-phase-dependent mobility of the lvh-encoding region in *Legionella pneumophila* strain Paris. Microbiology **152:**3561–3568. http://dx.doi.org/10.1099/mic.0.29227-0.
41. **Wee BA, Woolfit M, Beatson SA, Petty NK.** 2013. A distinct and divergent lineage of genomic island-associated Type IV Secretion Systems in Legionella. PLoS One **8**(12)**:**e82221. http://dx.doi.org/10.1371/journal.pone.0082221.
42. **Glockner G, Albert-Weissenberger C, Weinmann E, Jacobi S, Schunder E, Steinert M, Hacker J, Heuner K.** 2008. Identification and characterization of a new conjugation/type IVA secretion system (*trb/tra*) of *Legionella pneumophila* Corby localized on two mobile genomic islands. Int J Med Microbiol **298:**411–428. http://dx.doi.org/10.1016/j.ijmm.2007.07.012.
43. **Segal G, Russo JJ, Shuman HA.** 1999. Relationships between a new type IV secretion system and the icm/dot virulence system of *Legionella pneumophila*. Mol Microbiol **34:**799–809. http://dx.doi.org/10.1046/j.1365-2958.1999.01642.x.
44. **Ilangovan A, Connery S, Waksman G.** 2015. Structural biology of the Gram-negative bacterial conjugation systems. Trends Microbiol **23:**301–310. http://dx.doi.org/10.1016/j.tim.2015.02.012.
45. **Waldor MK.** 2010. Mobilizable genomic islands: going mobile with oriT mimicry. Mol Microbiol **78:**537–540. http://dx.doi.org/10.1111/j.1365-2958.2010.07365.x.
46. **Klebanoff SJ.** 2005. Myeloperoxidase: friend and foe. J Leukoc Biol **77:**598–625. http://dx.doi.org/10.1189/jlb.1204697.
47. **Andrews HL, Vogel JP, Isberg RR.** 1998. Identification of linked *Legionella pneumophila* genes essential for intracellular growth and evasion of the endocytic pathway. Infect Immun **66:**950–958.
48. **Berger KH, Merriam JJ, Isberg RR.** 1994. Altered intracellular targeting properties associated with mutations in the *Legionella pneumophila dotA* gene. Mol Microbiol **14:**809–822. http://dx.doi.org/10.1111/j.1365-2958.1994.tb01317.x.
49. **Molofsky AB, Shetron-Rama LM, Swanson MS.** 2005. Components of the *Legionella pneumophila* flagellar regulon contribute to multiple virulence traits, including lysosome avoidance and macrophage death. Infect Immun **73:**5720–5734. http://dx.doi.org/10.1128/IAI.73.9.5720-5734.2005.
50. **Rasis M, Segal G.** 2009. The LetA-RsmYZ-CsrA regulatory cascade, together with RpoS and PmrA, posttranscriptionally regulates stationary phase activation of *Legionella pneumophila* Icm/Dot effectors. Mol Microbiol **72:**995–1010. http://dx.doi.org/10.1111/j.1365-2958.2009.06705.x.
51. **Mukherjee S, Yakhnin H, Kysela D, Sokoloski J, Babitzke P, Kearns DB.**

2011. CsrA-FliW interaction governs flagellin homeostasis and a checkpoint on flagellar morphogenesis in *Bacillus subtilis*. Mol Microbiol **82:**447–461. http://dx.doi.org/10.1111/j.1365-2958.2011.07822.x.

52. **Bandyopadhyay P, Liu S, Gabbai CB, Venitelli Z, Steinman HM.** 2007. Environmental mimics and the Lvh type IVA secretion system contribute to virulence-related phenotypes of *Legionella pneumophila*. Infect Immun **75:**723–735. http://dx.doi.org/10.1128/IAI.00956-06.
53. **Miyamoto H, Yoshida S, Taniguchi H, Shuman HA.** 2003. Virulence conversion of *Legionella pneumophila* by conjugal transfer of chromosomal DNA. J Bacteriol **185:**6712–6718. http://dx.doi.org/10.1128/JB.185.22.6712-6718.2003.
54. **Vakulskas CA, Potts AH, Babitzke P, Ahmer BM, Romeo T.** 2015. Regulation of bacterial virulence by Csr (Rsm) systems. Microbiol Mol Biol Rev **79:**193–224. http://dx.doi.org/10.1128/MMBR.00052-14.
55. **Dubey AK, Baker CS, Romeo T, Babitzke P.** 2005. RNA sequence and secondary structure participate in high-affinity CsrA-RNA interaction. RNA **11:**1579–1587. http://dx.doi.org/10.1261/rna.2990205.
56. **Duss O, Michel E, NDiarra dit Konte Schubert M, Allain FH.** 2014. Molecular basis for the wide range of affinity found in Csr/Rsm protein-RNA recognition. Nucleic Acids Res **42:**5332–5346. http://dx.doi.org/10.1093/nar/gku141.
57. **Mercante J, Edwards AN, Dubey AK, Babitzke P, Romeo T.** 2009. Molecular geometry of CsrA (RsmA) binding to RNA and its implications for regulated expression. J Mol Biol **392:**511–528. http://dx.doi.org/10.1016/j.jmb.2009.07.034.
58. **Montero Llopis P, Jackson AF, Sliusarenko O, Surovtsev I, Heinritz J, Emonet T, Jacobs-Wagner C.** 2010. Spatial organization of the flow of genetic information in bacteria. Nature **466:**77–81. http://dx.doi.org/10.1038/nature09152.
59. **Berger KH, Isberg RR.** 1993. Two distinct defects in intracellular growth complemented by a single genetic locus in *Legionella pneumophila*. Mol Microbiol **7:**7–19. http://dx.doi.org/10.1111/j.1365-2958.1993.tb01092.x.
60. **Wiater LA, Sadosky AB, Shuman HA.** 1994. Mutagenesis of *Legionella pneumophila* using Tn*903* dlllacZ: identification of a growth-phase-regulated pigmentation gene. Mol Microbiol **11:**641–653. http://dx.doi.org/10.1111/j.1365-2958.1994.tb00343.x.
61. **Mukherjee S, Bree AC, Liu J, Patrick JE, Chien P, Kearns DB.** 2015. Adaptor-mediated Lon proteolysis restricts *Bacillus subtilis* hyperflagellation. Proc Natl Acad Sci U S A **112:**250–255. http://dx.doi.org/10.1073/pnas.1417419112.